STUDY ON APPLICATION OF CONTROLLABLE DAMPERS USING SMART MATERIALS TO FULL-SCALE BASE-ISOLATED BUILDINGS

E. Sato[1] and T. Fujita[2]

[1] *National Research Institute for Earth Science and Disaster Prevention, Hyogo, Japan*
[2] *Professor, Institute of Industrial Science, the University of Tokyo, Japan*
Email:eiji@bosai.go.jp, tfujita@iis.u-tokyo.ac.jp

ABSTRACT :
Many base-isolated buildings have been constructed using passive isolation systems with the purpose of reducing response accelerations of superstructures during earthquakes. However, there is a trade-off problem in a fact that large relative displacements are inevitable in the passive isolation systems to reduce the response accelerations of the superstructures. In order to solve this problem, semi-active seismic isolation systems with a controllable friction damper using piezoelectric actuators, a controllable friction damper using a hydraulic system driven by giant magnetostrictive actuators, and a controllable viscous damper using a magnetorheological (MR) fluid damper have been developed. We have shown in our previous studies that the effectiveness of these semi-active seismic isolation systems with the three abovementioned controllable dampers reduce the response accelerations and displacements. In our previous studies, we carried out the excitation tests using a small-scale structure model in order to confirm the effectiveness of these semi-active seismic isolation systems. However, in order to apply the three abovementioned controllable dampers to large structures, it is necessary to increase their capacity. In this study, the controllable dampers are applied to full-scale structures, and the expansion of each damper and performance of the semi-active isolation systems are examined by a numerical simulation. This paper outlines the expansion of these dampers and the simulation results for the seismic isolation effects; further, it summarizes the relative displacement reduction effects of the semi-active seismic isolation systems using the controllable dampers for full-scale buildings.

KEYWORDS:
Seismic Isolation, Semi-Active Control, Controllable Damper, Smart material, Full-Scale

1. INTRODUCTION

In order to reduce the response acceleration of superstructures during earthquakes, several base-isolated buildings have been constructed using passive isolation systems [1]. The disadvantage in this case is that large relative displacements are observed when the passive seismic isolation systems are used to reduce the response acceleration of the superstructures.
To solve this problem, semi-active seismic isolation systems that use controllable friction dampers have been developed [2].
On the other hand, in recent years, smart structures using smart materials have been actively researched in the field of architecture and civil engineering. Since smart structures can be used to realize compact, high-performance structures, they can be used in seismic control of large buildings and in health monitoring.
We have developed controllable dampers using smart materials for semi-active seismic isolation systems. [3],[4],[5]. In our previous studies, we performed excitation tests using a small seismic isolation test model and conducted numerical analyses, and thereby confirmed that the semi-active seismic isolation systems with a controllable friction damper using piezoelectric actuators, a controllable viscous damper using a magnetorheological (MR) fluid damper, and a controllable friction damper using a hydraulic system driven by giant magnetostrictive actuators can reduce the response acceleration and relative displacement. The generation force of these controllable dampers is less than or equal to 10 kN; hence, these controllable dampers cannot be applied to full-scale base-isolated buildings. Therefore, it is necessary to increase the capacity of the controllable dampers.

In this study, the controllable dampers are applied to the full-scale base-isolated buildings that are a high-rise, a medium-rise, and a low-rise building, and the expansion of each damper and performance of the semi-active isolation systems using the extended controllable dampers are examined by numerical simulation.

2. FULL-SCALE BUILDING MODELS

For examining the feasibility of applying semi-active seismic isolation systems with the controllable dampers using the smart materials to the full-scale base-isolated buildings, the targeted building models were considered to be of three types: high-rise, medium-rise, and low-rise building models. The examined building models are described in the following sections.

2.1. High-Rise Building Model

A 30-story steel structure building was considered as the high-rise building model. Table 1 and Figure 1 show the main specifications and schematic diagram of this high-rise building model, respectively.

Table 1 Main specifications of high-rise building model

Items	Specifications
Story (structure)	30 (steel)
Height (floor height)	111.5 m (3.7 m(1F 4.2 m))
Floor area	1576.96 m^2(44.8 m × 35.2 m)
Mass(superstructure)	31000 ton
First period of the superstructure	2.8 s
Isolation period	5 s

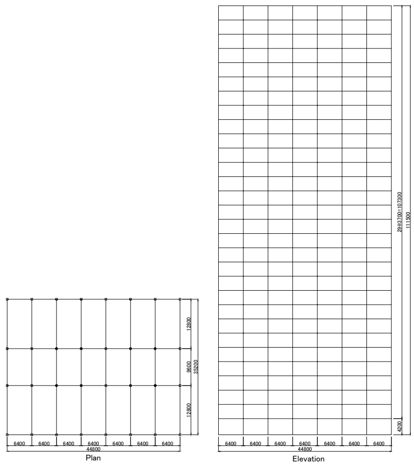

Figure 1 Schematic diagram of high-rise building model

2.2. Medium-Rise Building Model

A 16-story steel structure building was considered as the medium-rise building model. Table 2 and Figure 2 show the main specifications and the schematic diagram of this medium-rise building model, respectively.

Table 2 Main specifications of medium-rise building model

Items	Specifications
Story (structure)	16 (steel)
Height (floor height)	65 m(4 m(1F 5 m))
Floor area	200.34 m^2(12.6 m × 15.9 m)
Mass(superstructure)	3345 ton
First period of the superstructure	1.86 s
Isolation period	3.5 s

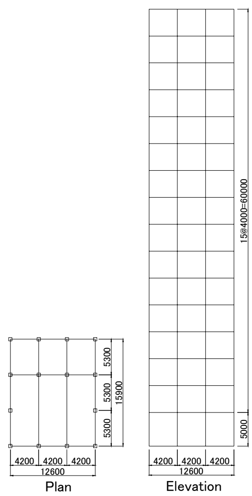

Figure 2 Schematic diagram of medium-rise building model

2.3. Low-Rise Building Model

A 3-story reinforced concrete structure building was considered as the low-rise building model. Table 3 and Figure 3 show the main specifications and schematic diagram of this low-rise building model, respectively.

Table 3 Main specifications of low-rise building model

Items	Specifications
Story (structure)	3 (RC)
Height (floor height)	11 m(3.5 m(1F 4 m))
Floor area	1420.8 m^2(64 m × 22.2 m)
Mass(superstructure)	5840 ton
First period of the superstructure	0.13 s
Isolation period	3 s

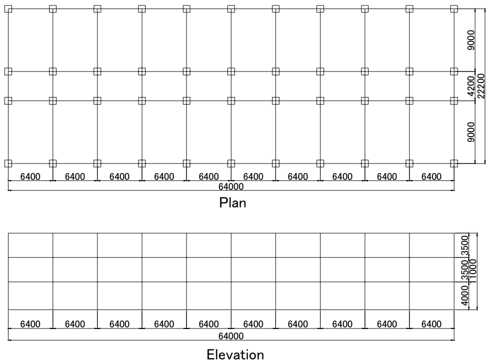

Figure 3 Schematic diagram of low-rise building model

3. EXAMINATION OF THE REAL SCALE DUMPERS

In order to use the passive damper, the controllable friction damper using the piezoelectric actuators, the MR damper and the controllable friction damper using the hydraulic system driven by the giant magnetostrictive actuators for the full-scale base isolation buildings, their basic specifications are designed, and the practicality of each damper is evaluated.

3.1. Passive Damper

The oil damper whose damping force is proportional to the velocity of a slider was considered as a passive damper. The damping force of the oil damper is 500 kN, which is the standard capacity. Table 4 shows the number of oil dampers (approximately 20% damping ratio) that are set in the three abovementioned building models.

Table 4 Number of oil dampers in the three building models
(damping ratio is 20%)

Type	Number of dampers	Damping coefficient ×10^3[kN s/m]
30	39	15.6
16	6	2.4
3	12	4.8

3.2. Expansion of the Controllable Friction Damper Using the Piezoelectric Actuators

The basic parameters of the controllable friction damper using the piezoelectric actuators are set; this damper can generate a friction force of 500 kN, similar to the damping force of the oil damper for the passive seismic isolation system. Table 5 shows the desired specifications of this controllable friction damper.

When the generation efficiency of the piezoelectric actuators and backlash of the controllable friction damper are considered, a piezoelectric actuator that generates a force of 3000 kN is required. Table 6 shows the design specifications of such a piezoelectric actuator. However, by considering the previous manufacturing experiences, the manufacturing of this piezoelectric actuator is very difficult.

The schematic diagram of the controllable friction damper that generates a friction force of 500 kN is shown in Figure 4.

Table 5 Desired specifications of this controllable friction damper

Items	Specifications
Friction force [kN]	0-500
Friction coefficient	0.25
Initial pressure [kN]	1000
Number of the piezoelectric actuator	4
Needful releasing force (for one) [kN]	250

Table 6 Design specifications of piezoelectric actuator

Items	Specifications
Drive voltage [V]	2000
Size [mm](W × D × H)	300 × 300 × 163
Max. displacement [μm]	150
Max. force [kN]	3000
Stack number	88
Stack thickness [mm]	1.85
Electric capacity [μF]	159
Electric field [V/mm]	1081
Max. strain [μst]	921.4
Stress [MPa]	33.3
Young's modulus [kN/m^2]	36.2 × 10^9
Max. current [A](at 10 Hz)	20.0

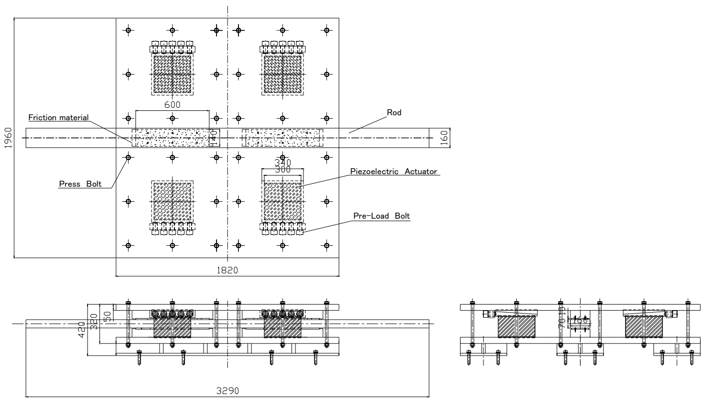

Figure 4 Schematic diagram of controllable friction damper using piezoelectric actuators

3.3. Expansion of the MR Damper

The basic parameters of the MR damper that can generate a damping force of 500 kN are set. Table 7 shows the specifications of the designed MR damper. Further, the relationship between the damping force and the velocity of the sliding rod is shown in Figure 5. Therefore, it is confirmed that an MR damper generating a damping force of 500 kN can be achieved.

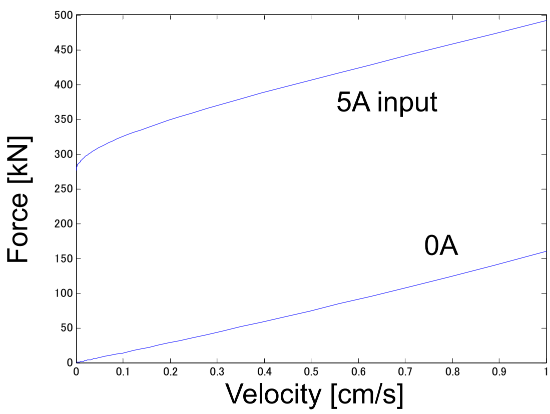

Figure 5 Relationship between the damping force and the velocity of slideing rod

Table 7 Specifications of designed MR damper

Items		Designed value
Max. damping force [kN]		500
Cylinder bore [mm]		φ170
Piston's outside diameter [mm]		φ100
Bypass	Outside diameter [mm]	φ80
	Inside diameter [mm]	φ76
	Length [mm]	310
MR fluid	Maker	LORD-MRF-132LD
	Density [kg/m^3]	3055
	Viscosity [s^{-1}]	0.33
Electro-magnet	Coil	272winding×10
	Inductance [mH]	60
	Resistance [Ω]	10
	Current [A]	5
Damping coefficient [kN s/m] (in the absence of a magnetic field)		155.7

3.4. Expansion of the Controllable Friction Damper Using the Hydraulic System Driven by the Giant Magnetostrictive Actuators

The basic parameters of the controllable friction damper using the hydraulic system driven by the giant magnetostrictive actuator are set, and this damper can generate a damping force of 500 kN. Table 8 shows the specifications of the designed friction damper. A friction force of 500 kN is achieved by using two double-piston brakes. The inner diameter and outer diameter of one piston of the brake are 10 cm and 22.31 cm, respectively. Figure 6 shows the schematic diagram of this friction damper.

Table 8 Specifications of designed controllable friction damper using hydraulic system driven by a giant magnetostrictive actuator

Items	Specification
Friction force [kN]	0-500
Friction coefficient	0.25
Max. oil pressure [MPa]	8
Brake	
Type	Negative brake
Number of piston	4
Area presented to the wind [cm^2] (for a single piston)	312.5
Inner diameter [cm] (for a single piston)	10
Outer diameter [cm] (for a single piston)	22.31

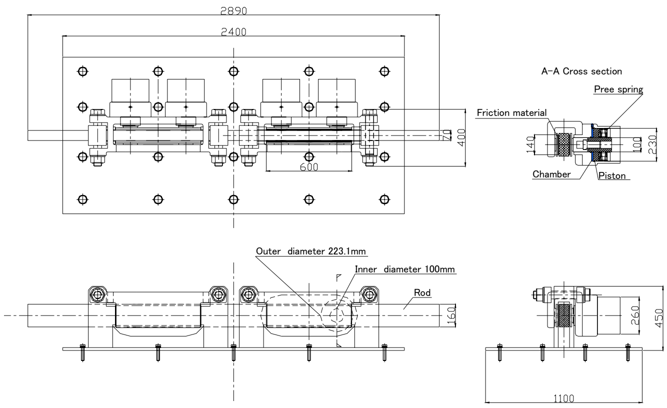

Figure 6 Schematic diagram of controllable friction damper using hydraulic system driven by giant magnetostrictive actuator

3.5. Summary of the Expansion of the Controllable Dampers

The expansion of the controllable friction damper using the piezoelectric actuators, MR damper, and controllable friction damper using the hydraulic system driven by the giant magnetostrictive actuators were examined in order to apply to the full-scale base-isolated buildings. A standard damping force of 500 kN was considered as the target value, and then, the specifications of these controllable dampers were designed. Consequently, it was confirmed that the controllable friction damper using the piezoelectric actuators is not suitable for practical use. Since the size of the piezoelectric actuator is considerably large (300 × 300 × 163 mm),

its manufacture appears to be very difficult on considering the previous manufacturing experiences; further, this actuator generates a damping force of 3000 kN.
Thereafter, the response analyses for the semi-active seismic isolation buildings with the MR damper and controllable friction damper using the hydraulic system driven by the giant magnetostrictive actuators were conducted for the full-scale base-isolated buildings (high-rise, medium-rise, and low-rise buildings).

4. NUMERICAL SIMULATION

4.1. Conditions for the Numerical Simulation

The MR damper and controllable friction damper using the hydraulic system driven by the giant magnetostrictive actuators were set as the controllable dampers of the semi-active seismic isolation systems. Further, the high-rise (30-story building), medium-rise (16-story building) and low-rise building (3-story building) were considered as the full-scale base-isolation building models. The short-period waves that were input were El Centro NS (1940, Imperial Valley Earthquake), JMA NS (1995, Hyogoken-Nanbu Earthquake), Hachinohe NS (1968, Tokachi-Oki Earthquake), and Taft EW (1952, Arvin-Tehachapi Earthquake). On the other hand, the long-period wave that was input was Tomakomai EW (2003, Tokachi-Oki Earthquake). The velocity levels of the short-period waves were set to 25 and 50 cm/s, and the long-period wave was set to the real scale. The semi-active control law used Linear Quadratic optimum regulator theory (LQ). The simulations were conducted with the controllers that were designed to reduce response acceleration (case1) and relative displacement (case2).

4.2. Results of the Numerical Simulation

The results obtained for the high-rise, medium-rise, and low-rise building models are shown in Figures 7-8, in Figures 9-10 and in Figures 11-12, respectively. Owing to the space constraints, the results of El Centro NS and Tomakomai EW are shown here.
The desired effect of the semi-active seismic isolation systems using the MR damper and controllable friction damper on the high-rise and medium-rise buildings was not achieved for the short-period waves. The reason for this is that the response acceleration and relative displacement are sufficiently reduced by using the passive seismic isolation system because the isolation period of the buildings is set to be sufficiently long for short period waves.
On the other hand, the response acceleration and relative displacement of the high-rise and medium-rise buildings are reduced to approximately 90% or more for the long-period wave Tomakomai EW compared with that of the passive seismic isolation systems
Next, in the case of the low-rise building, the effectiveness of the semi-active seismic isolation systems using both the dampers is shown for the short- and long-period waves. The relative displacement is reduced to approximately 60%, and the response acceleration is reduced to approximately 90% compared with the passive seismic isolation systems.
Moreover, the semi-active seismic isolation system using the MR damper reduced the responses compared with that using the controllable friction damper using the hydraulic system driven by the giant magnetostrictive actuators. The relative displacement and response acceleration in the semi-active seismic isolation system with the MR damper are reduced to 95% compared with those vales in the semi-active seismic isolation system with the controllable friction damper using the hydraulic system driven by the giant magnetostrictive actuators

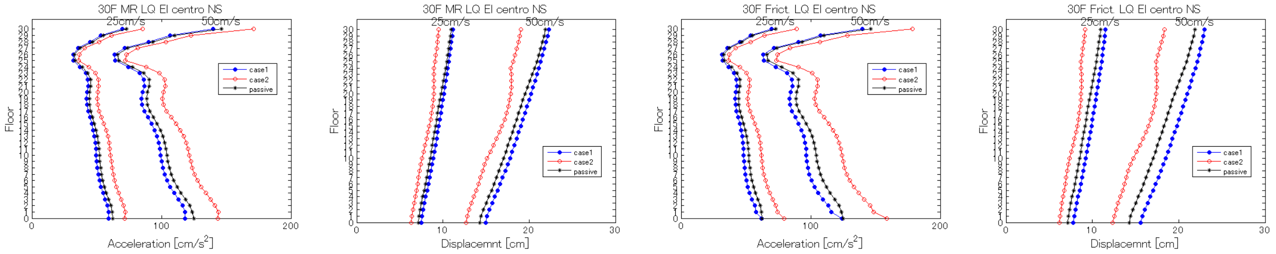

Resp. Acc. Rel. Disp. Resp. Acc. Rel. Disp.

(a) Using MR damper (b) Using controllable friction damper

Figure 7 Results obtained when El Centro NS (short-period wave) is input to the high-rise building

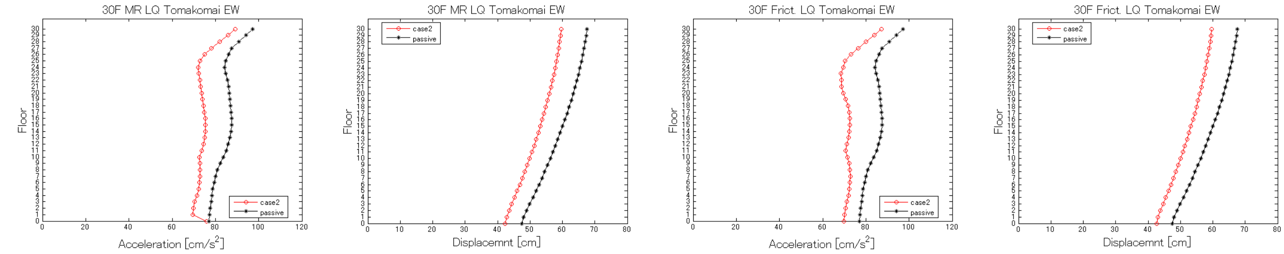

Resp. Acc. Rel. Disp. Resp. Acc. Rel. Disp.

(a) Using MR damper (b) Using controllable friction damper

Figure 8 Results obtained when TOMAKOMAI EW (long-period wave) is input to the high-rise building

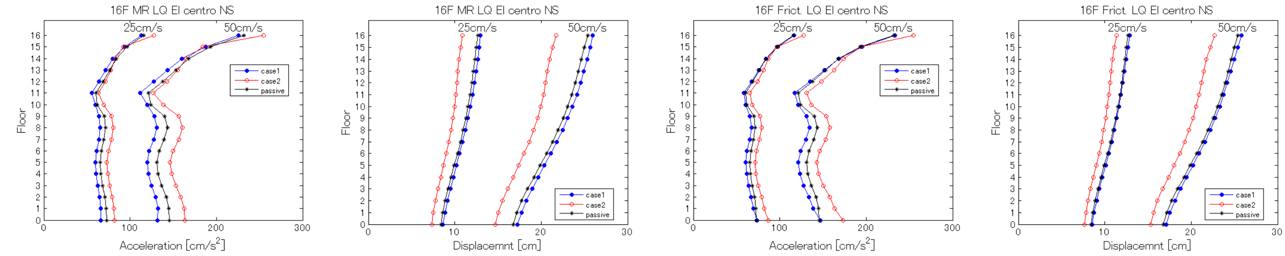

Resp. Acc. Rel. Disp. Resp. Acc. Rel. Disp.

(a) Using MR damper (b) Using controllable friction damper

Figure 9 Results obtained when El Centro NS (short-period wave) is input to the medium-rise building

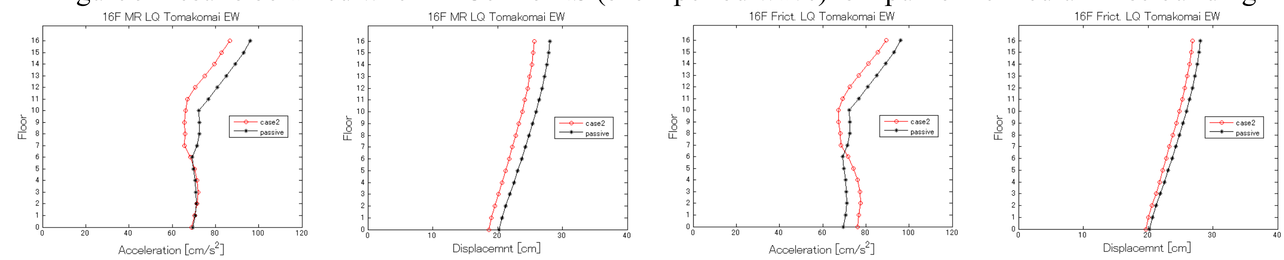

Resp. Acc. Rel. Disp. Resp. Acc. Rel. Disp.

(a) Using MR damper (b) Using controllable friction damper

Figure 10 Results obtained when TOMAKOMAI EW (long-period wave) is input to the medium-rise building

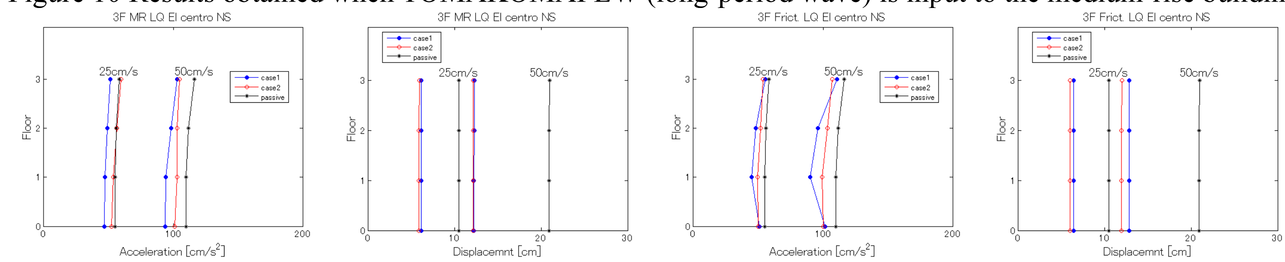

Resp. Acc. Rel. Disp. Resp. Acc. Rel. Disp.

(a) Using MR damper (b) Using controllable friction damper

Figure 11 Results obtained when El Centro NS (short-period wave) is input to the low-rise building

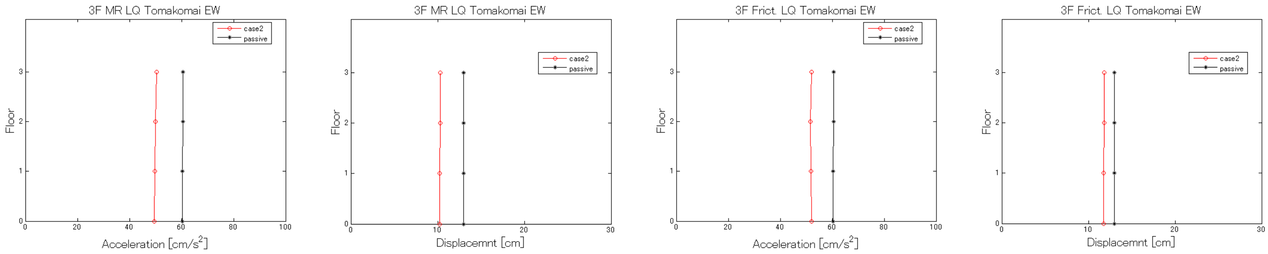

Resp. Acc. Rel. Disp. Resp. Acc. Rel. Disp.

(a) Using MR damper (b) Using controllable friction damper

Figure 12 Results obtained when TOMAKOMAI EW (long-period wave) is input to the low-rise building

5. CONCLUSIONS

In order to apply semi-active seismic isolation systems to full-scale base-isolation buildings, the expansion of the three controllable dampers was examined. Therefore, it was confirmed that the controllable friction damper using piezoelectric actuators is not suitable for practical use.

Response analyses of the semi-active seismic isolation buildings with the MR damper and controllable friction damper using the hydraulic system driven by the giant magnetostrictive actuators were performed for full-scale base-isolation buildings (high-rise, medium-rise and low-rise buildings). Consequently, the desired effect of the semi-active seismic isolation systems using these controllable dampers on the high-rise and medium-rise buildings was not achieved for the short-period waves, however, the desired effect of the semi-active seismic isolation systems using these controllable dampers on the high-rise and medium-rise buildings was achieved for the long-period wave.

On the other hand, in the case of the low-rise building, the desired effect of the semi-active seismic isolation system using these dampers was sufficiently achieved for the short- and long-period waves.

Moreover, it was confirmed that the semi-active seismic isolation system using the MR damper is the most effective system.

REFERENCES

[1] Fujita, T. (1991), Research, development and application of seismic isolation systems in Japan, Proceeding of the International Meeting on Earthquake Protection of Builgings, Ancona, Italy,6-8, June, 77/C-90/C.

[2] Fujita, T., Kabeya, K., Hayamizu, Y., Aizawa, S., Higashino, M., Kubo, T., Haniuda, N., and Mori, T., (1991b), Semi-active seismic isolation system using controllable friction damper (1st report, Development of controllable friction damper and fundamental study of semi-active control system), *Transactions of the Japan Society of Mechanical Engineers, Series C*, Vol. 57, No. 536, pp. 1122-1128 (in Japanese).

[3] Sato, E., Fujita, T. (2005) Semi-Active Seismic Isolation System with Controllable Friction Dampers Using Piezoelectric Actuators. *Transactions of the Japan Society of Mechanical Engineers, Series C*, Vol. 71,No. 702, pp. 405-412. (in Japanese)

[4] Sato, E., Fujita, T. (2006) Semi-Active Seismic Isolation System with Controllable Viscous Dampers Using Magneto-Rheological Fluid, *Transactions of the Japan Society of Mechanical Engineers, Series C*, Vol. 72, No. 717, pp. 1428-1434. (in Japanese)

[5] Sato, E., Fujita, T. (2007), Semi-Active Seismic Isolation System with Controllable Friction Dampers Using Hydraulic System Driven by Giant Magnetostrictive Actuators, *Transactions of the Japan Society of Mechanical Engineers, Series C*, Vol. 73,No. 730, pp. 1723-1730. (in Japanese)